ResearchGate

See discussions, stats, and author profiles for this publication at: https://www.researchgate.net/publication/221894839

Triple Stimulus–Responsive Polypeptide Nanoparticles That Enhance Intratumoral Spatial Distribution

ARTICLE *in* NANO LETTERS · MARCH 2012

Impact Factor: 13.59 · DOI: 10.1021/nl300630c · Source: PubMed

CITATIONS
35

READS
18

8 AUTHORS, INCLUDING:

Wenge Liu
Duke University
44 PUBLICATIONS **1,518** CITATIONS
SEE PROFILE

Xinghai Li
Duke University
231 PUBLICATIONS **1,790** CITATIONS
SEE PROFILE

Matthew R Dreher
National Institutes of Health
64 PUBLICATIONS **2,946** CITATIONS
SEE PROFILE

Ashutosh Chilkoti
Duke University
292 PUBLICATIONS **15,049** CITATIONS
SEE PROFILE

Available from: Ashutosh Chilkoti
Retrieved on: 02 February 2016

NIH Public Access
Author Manuscript
Nano Lett. Author manuscript; available in PMC 2013 April 11.

Published in final edited form as:
Nano Lett. 2012 April 11; 12(4): 2165–2170. doi:10.1021/nl300630c.

Triple stimulus-responsive polypeptide nanoparticles that enhance intratumoral spatial distribution

Daniel J. Callahan[1,2], **Wenge Liu**[1], **Xinghai Li**[1], **Matthew R. Dreher**[3], **Wafa Hassouneh**[1,2], **Minkyu Kim**[2,4], **Piotr Marszalek**[2,4], and **Ashutosh Chilkoti**[1,2,*]

[1]Department of Biomedical Engineering, Duke University, 136 Hudson Hall, Box 90281, Durham NC, 27708

[2]Center for Biologically Inspired Materials and Material Systems, Duke University, Box 90300, Durham, NC, 27708

[3]Center for Interventional Oncology, Clinical Center, National Cancer Institute, National Institutes of Health, 9000 Rockville Pike, Bethesda, MD, 20892

[4]Department of Mechanical Engineering and Materials Science, Duke University, Box 90300, Durham, NC, 27708

Abstract

To address the limited tumor penetration of nanoparticle drug delivery vehicles, we report the first pH-responsive polypeptide micelle that dissociates at the low extracellular pH of solid tumors. This histidine-rich elastin-like polypeptide block copolymer (ELP_{BC}) self-assembles at 37°C into spherical micelles that are stabilized by Zn^{2+} and are disrupted as the pH drops from 7.4 to 6.4. These pH-sensitive micelles demonstrate better *in vivo* penetration and distribution in tumors than a pH-insensitive control.

Keywords

polypeptides; block copolymers; stimulus-responsive; pH responsive; tumor drug delivery

Self-assembled polymer nanoparticles are of interest for cancer therapy and imaging because: [1] self-assembly provides a facile method for the bottom-up synthesis of sub-100 nm size nanoparticles of tunable size and interfacial properties; [2] these particles can exploit the enhanced permeability and retention effect –a consequence of the leaky vasculature of many solid tumors and the absence of a functional lymphatic system– to accumulate in tumors;[1] and [3] these particles can be designed to carry useful payloads such as low molecular weight chemotherapeutics or imaging agents in the core or exterior by chemical conjugation to the polymer constituents[2] or physical encapsulation.[3-6] Despite their promise for cancer therapy and imaging, the effectiveness of nanoparticulate carriers is limited by their poor penetration into tumor tissue.[7] This is because the dense extracellular matrix, dense cell packing, and high interstitial fluid pressure in solid tumors limits their transport, so that most nanoparticles are unable to distribute homogeneously throughout the

*chilkoti@duke.edu.

Supporting Information Available Experimental methods and supplementary data characterizing the effect of transition metals on single block ELP T_t, the specificity of pH-responsiveness to histidine-rich ELPs, the reversibility of Zn^{2+} stabilization, tumor pH, ELP_{BC} biodistribution, supplementary autoradiographic images, and an SDS-PAGE gel demonstrating the identity and purity of the synthesized ELPs. This material is available free of charge via the Internet at http://pubs.acs.org

NIH-PA Author Manuscript
NIH-PA Author Manuscript
NIH-PA Author Manuscript

NIH-PA Author Manuscript

NIH-PA Author Manuscript

NIH-PA Author Manuscript

tumor and instead accumulate principally in the perivascular region after systemic administration.[8]

Stimulus-responsive polymer nanoparticles could address this problem because they can be designed to undergo a tumor-specific material transition that can lead to their programmed disassembly within a tumor, thereby releasing their lower molecular weight constituents that can more readily diffuse within the tumor. Motivated by this rationale, we report herein a pH-sensitive, recombinant diblock peptide polymer that exhibits self-assembly at pH 7.4 and low pH-triggered disassembly at pH 6.4 as shown in the Table-of-Contents figure accompanying the abstract. We chose this narrow range of pH as the trigger of interest because it corresponds to the difference in extracellular pH between normal tissue (7.2–7.4) and many solid tumors (pH 6.2-6.9) resulting from hypoxia, anaerobic respiration, and ion channel disregulation.[9]

Our design is based on thermally responsive elastin-like polypeptides (ELPs), a class of peptide polymers composed of a VPGXG repeat that exhibit lower critical solution temperature (LCST) phase transition behavior.[10] Building on previous work in our laboratory demonstrating that ELP block copolymers (ELP_{BC}s) consisting of blocks with significantly different LCSTs can form spherical micelles over a specific range of temperature,[11] we designed ELP_{BC}s with histidine-rich hydrophobic blocks to create pH-responsive nanoparticles. We show that these systems self-assemble in response to the three orthogonal triggers of temperature, pH and co-solutes: temperature can be used to self-assemble the ELP_{BC}s into micelles below physiological temperature, a drop in pH that corresponds to tumor pH leads to micelle disassembly, and addition of physiological concentrations of Zn^{2+} can further stabilize these micelles or alternatively can be used to trigger their self-assembly at lower temperatures with no adverse impact on their pH sensitivity. These micelles are the first example of a pH-responsive polypeptide nanoparticle precisely tuned to disassemble at the extracellular pH encountered in solid tumors. Furthermore, we demonstrate for the first time how such a pH-sensitive nanoparticle can achieve a more homogeneous intratumoral spatial distribution than its pH-insensitive counterpart, suggesting the potential utility of pH-responsive polypeptide nanoparticles for the improved delivery of drugs or imaging agents to solid tumors.

Our design of an ELP capable of displaying pH-modulated self-assembly between pH 7.4 and 6.4 began with the twin observations that charge modulation alters the phase transition behavior of ELPs[12,13] and that His guest residues (X in the VPGXG repeat) should lead to the most sensitive response in the pH range of 7.4 to 6.4 because His has the pK_a closest to 7.4 of any amino acid. To explore the pH sensitivity of His-containing ELPs, we synthesized two sets of His-containing single segment ELPs: ELP[VH_2GA]-*n*,[14] which contains V, H, G and A guest residues in a 1:2:1:1 ratio and where the number of pentapeptide repeats *n* varies from 40-120; and ELP[VH_4]-*n*, where *n* varies from 40 to 100. The transition temperature (T_t) of these His-rich ELPs increases at low pH due to the evolution of positive charges on the histidine residues, making the ELP more hydrophilic, thus decreasing the entropic penalty for solvation and increasing the temperature required for desolvation to become energetically favorable (Figure 1A). pH had a greater effect on the T_t of ELP[VH_4]-80 than that of ELP[VH_2GA]-60, consistent with the higher concentration of histidine residues in this ELP, with the T_t of [VH_4]-80 showing a dramatic increase from ~30 °C at pH 7.4 to ~60 °C at pH 6.4, the pH range of physiological interest. The small difference in MW of these ELPs cannot explain the difference in their pH-responsiveness, as indicated by our previous characterization of the effect of molecular parameters on the phase behavior of ELPs.[14-16]

NIH-PA Author Manuscript

NIH-PA Author Manuscript

NIH-PA Author Manuscript

We next investigated the sensitivity of the LCST phase transition of these ELPs to transition metal concentration, as histidine is known to coordinate with the transition metals Co^{2+}, Cu^{2+}, Ni^{2+}, and Zn^{2+}.[17,18] A dramatic decrease in the T_t of ELP[VH_2GA]-60 was observed in the presence of μM concentrations of $CoCl_2$, $CuCl_2$, $NiCl_2$, and $ZnCl_2$, while at least 500 mM concentrations of NaCl, KCl, $CaCl_2$, $MgCl_2$, $MnCl_2$, and $FeCl_2$ were required to induce a decrease (Figure S1). These results indicate that the decrease in T_t induced by Co^{2+}, Cu^{2+}, Ni^{2+} or Zn^{2+} is not the result of the Hofmeister effect[19] or of a non-specific divalent cation-dependent effect, but instead depends on the specific coordination of these metal cations with histidine side-chains.

Next, we synthesized a series of ELP_{BC}s with hydrophilic, pH-insensitive blocks (intended to form the corona of the micelle) and hydrophobic, pH-sensitive blocks to form the core of the micelles. ELP[$V_1G_7A_8$] was chosen as the pH-insensitive hydrophilic coronal block based on its T_t above physiological temperature.[20] We synthesized a variety of ELP_{BC}s with [VG_7A_8] corona blocks and [VH_2GA] or [VH_4] core blocks, generally keeping the hydrophilic:hydrophobic block length ratio in the range of 1:2 to 2:1, based on a previous study that showed that block ratios in this size range lead to self-assembly into micelles.[11] The ELP_{BC}s were screened for micelle formation by spectrophotometry and dynamic light scattering (DLS). [VG_7A_8]-80/[VH_4]-100 was selected for further analysis because it was the only ELP_{BC} that formed stable nanoparticles in the physiological range of temperature.

DLS of [VG_7A_8]-80/[VH_4]-100 at pH 7.4 (Figure 1B) demonstrated three-state behavior as a function of temperature; at temperatures below 32 °C, an R_h of 7 nm was observed, consistent with the size of soluble unimers of the ELP_{BC}. Between 32 and 39 °C, particles with an R_h of ~35 nm were observed, and raising the temperature above 40 °C led to the formation of micron-sized aggregates (not shown in Figure 1B due to the inaccuracy of light scattering measurements in this size range). Just as for pH-insensitive ELP block copolymers,[11] the two ELP blocks have sufficiently different transition temperatures that they transition independently, leading to a monomer-to-micelle transition at an intermediate temperature referred to as the critical micelle temperature (CMT), 32 °C in this case, and then a micelle-to-aggregate transition at a higher temperature of 39 °C.

These ELP_{BC}s are exquisitely pH-sensitive (Figure 1B); at pH 6.8, micelle formation was only observed over a narrow range of temperature, while only a single monomer-to-aggregate transition was observed at pH 6.4 and pH 6.0. No unimer-to-micelle transition occurred at low pH because as the histidine-rich block becomes increasingly hydrophilic the T_ts of the two blocks approach one another, leading to a single monomer-to-aggregate transition. The data in Figure 1B clearly show that there is a range of temperatures from 32 to 39 °C where decreasing the pH from 7.4 to 6.4 disassembles preformed micelles. Isothermal pH cycling further confirmed the rapid and reversible disassembly of micelles in response to a decrease in pH (Figure 1C). DLS of a His-free ELP_{BC} showed no change in its R_h with a change in pH, confirming that the pH-sensitivity of these nanoparticles arises from the histidine residues in the hydrophobic block (Figure S2).

Next, we examined the effect of $ZnCl_2$ on the histidine-rich ELP_{BC}. $ZnCl_2$ was chosen for these experiments because Zn^{2+} is a relatively non-toxic metal ion,[21] with a physiological concentration of ~20 μM[22] and a tolerable upper intake level of 40 mg/day in humans, corresponding to a plasma concentration of roughly 200 μM.[21] DLS of [VG_7A_8]-80/[VH_4]-100 in HEPES revealed a decrease in the CMT from ~32 °C in the absence of $ZnCl_2$ to ~20 °C at 25 μM $ZnCl_2$ (Figure 1D) and to 5 °C at higher $ZnCl_2$ concentrations of 100 μM and 1 mM. $ZnCl_2$ increases the range of temperature over which micelles are stable because the increase in the hydrophobicity of the His-containing core-block upon chelation of Zn^{2+} leads to a higher entropic gain upon release of water molecules bound to the

NIH-PA Author Manuscript

NIH-PA Author Manuscript

NIH-PA Author Manuscript

hydrophobic segment and thus a lower CMT. The ELP_{BC} remains pH-sensitive in the presence of 25 μM $ZnCl_2$ (Figure S3A), and $ZnCl_2$ addition below the CMT rapidly leads to micelle assembly that can be reversed by chelation with EDTA (Figure S3B). The effect of $ZnCl_2$ depends on interactions with histidine side chains, as demonstrated by the lack of an effect on a His-free ELP_{BC} (Figure S3C).

We also investigated micelle stability by measuring the critical micelle concentration (CMC) using the pyrene fluorescence method. Increasing the pH from 7.4 to 8.0 yields an appreciable but statistically insignificant decrease in the CMC (from 32.6 ± 3.8 M to 23.7 ± 4.2 μM; $p>0.05$, t-test; Table 1). $ZnCl_2$ had a much greater effect on the CMC than pH, with a four-fold decrease at 100 μM $ZnCl_2$ and a nine-fold decrease at 1 mM $ZnCl_2$ ($p<0.01$ for both $ZnCl_2$ concentrations and both pHs, t-test). The increased stability of Zn^{2+}-loaded micelles is consistent with the increased hydrophobicity of the histidine-rich core-forming block in the presence of Zn^{2+}.

The morphology of these histidine-rich micelles were investigated by static light scattering (SLS) and tapping mode atomic force microscopy (AFM) in buffer. Analysis of the SLS data (Table 2; see SI for details) provided the radius of gyration (R_g), which when combined with the R_h independently determined by DLS provides the shape factor ($\rho = R_g/R_h$), which describes the morphology of the nanoparticles. The ρ values range from 0.5-0.62 for the ELP_{BC} nanoparticles (Table 2). These values are lower than the ideal value of 0.775 for spherical particles, but are consistent with a spherical morphology.[23] The Z value (number of polymer chains per particle) increased in the presence of Zn^{2+} and the ρ value decreased indicating a greater concentration of mass at the core, consistent with the increased stability as measured by the lower CMT and CMC of Zn^{2+}–stabilized micelles compared to micelles that were assembled in the absence of Zn^{2+}. Tapping mode AFM of zinc-stabilized micelles in buffer clearly revealed monodisperse, spherical particles with a diameter of ~60 nm, consistent with the light scattering results (Figure 1E).

Together, these results clearly show that the effects of temperature, pH, and Zn^{2+} on the self-assembly of this ELP_{BC} are orthogonal, with their triple environmental sensitivity summarized in Figure 1F. Raising the solution temperature from ambient to 37 °C leads to temperature-triggered self-assembly, pH provides a convenient trigger to disassemble these micelles in the range of tumor extracellular pH, and physiological concentrations of Zn^{2+} stabilize the micelles by lowering their CMT and CMC without affecting their pH-sensitivity.

We next examined the *in vivo* behavior of the histidine-rich ELP_{BC} in nude mice bearing human tumor xenografts. A pH-insensitive ELP control $[VG_7A_8]$-64/[V]-120 was selected because it exists as a micelle at 37 °C with a CMC that is similar to Zn^{2+} stabilized micelles of $ELP_{BC}[VG_7A_8]$-80/$[VH_4]$-100], but it does not disassemble in response to low pH (Figure S2), allowing it to serve as a negative control for the effect of extracellular tumor pH on the tumor biodistribution of the pH-sensitive micelles.[11] ^{125}I-labeled His-rich $[VG_7A_8]$-80/$[VH_4]$-100] and the His-free control $[VG_7A_8]$-64/[V]-120 were then injected *i.v.* into HCT-15 tumor-bearing nude mice to assess their biodistribution and intratumoral spatial distribution. This xenograft was selected based on a screening study wherein we measured the intratumoral pH of a set of human tumor xenografts in nude mice (Figure S4) and found that this tumor showed a reproducible sub-physiological pH of ~6.8, which could be further decreased to 6.3-6.6 by *i.p.* co-injection of glucose and *m*-iodobenzylguanidine (MIBG).[24]

Biodistribution results collected over 48 h indicate that both polymers exhibit key features associated with high molecular weight drug carriers (Figure S5). First, accumulation in healthy tissues is limited with the exception of the thyroid, which is an artifact of this

NIH-PA Author Manuscript

NIH-PA Author Manuscript

NIH-PA Author Manuscript

organ's preferential uptake of iodine (Figures S5A and S5B). Second, the persistence of significant amounts of polymer in the blood at 8 and 24 h following injection (Figure S5C) demonstrate that these carriers have a prolonged circulation time compared with small molecule drugs, thus allowing for gradual accumulation in the tumor. Third, tumor accumulation data (Figure 2A) show that approximately 4% /g of the injected dose reaches the tumor 8 h following injection, in the typical range of tumor accumulation for high molecular weight carriers, and that pH-sensitivity does not affect tumor accumulation. Taken together, these results demonstrate that both His-rich and His-free ELP_{BC}s retain the benefits of high molecular weight drug carriers.

Autoradiographic imaging of tumor sections revealed that pH-sensitive ELP_{BC}s achieved a more homogeneous spatial distribution within the tumor compared with the pH-insensitive control (Figures 2B and S6). Note that the two polymers had different degrees of radiolabeling so the intensities should not be compared. While the pH-insensitive polymer is concentrated in a small region, generally at the periphery of the tumor, the pH-sensitive histidine-rich ELP_{BC} exhibits a more diffuse distribution extending through the tumor volume. This difference is most obvious at 4 h, but persists over the time course studied here. The change in intratumoral spatial distribution based on pH-sensitivity was quantified in two ways. First, the homogeneity of tumor distribution was quantified as the coefficient of variation (CV) and compared between $[VG_7A_8]$-80/$[VH_4]$-100 (pH-sensitive ELP_{BC}) and $[VG_7A_8]$-64/[V]-120 (pH-insensitive control ELP_{BC}). The pH-sensitive polymer had a lower CV at all three time points tested here (Table S1), and this difference was statistically significant ($p = 0.05$) at 4 h post-injection with a ~30% lower CV of 0.216 ± 0.018 for the pH-sensitive ELP_{BC} versus 0.279 ± 0.033 for the pH-insensitive ELP_{BC}. Comparing CV accounts for the difference in intensity between the two polymers, and the normal distribution of intensities observed for both polymers suggests that this analysis is not affected by sub-threshold signal for the lower-intensity polymer (Figure S6B).

Second, the tumor penetration of the ELP_{BC}s was quantified using a custom image processing script to obtain the background-corrected intensity (normalized to the mean intensity of the tumor section) as a function of Euclidean distance from the tumor surface (Figure 2C). The pH-sensitive ELP_{BC} shows a more homogenous distribution in this analysis also, with significantly greater penetration to the tumor center (defined as the inner quarter of the tumor) for the pH-sensitive case at 4 h (t-test, $p < 0.05$). No difference in penetration was observed at 8 or 24 h post-injection.

To rule out other factors besides pH-sensitivity that could account for these results or affect their analysis, we first focused on the potential for a difference in vascular density between the two groups of animals. Immunostaining of tumor sections by a CD31-specific antibody that is specific for blood vessels demonstrated that this result is not an artifact of tumor vascularity, as no difference in microvessel density was observed between the two groups of tumors. Furthermore, the size of the pH-sensitive micelles and pH-insensitive controls (Figure 1 and reference 25), their stability at physiological pH as determined by their CMC at pH 7.4 (Table 1 and reference 25), their pharmacokinetics (Figure S5) and their overall level of accumulation in tumors (Figure 2A) are all very similar, suggesting that structural differences between the pH-responsive and pH-insensitive micelles –with the exception of their pH-sensitivity– are not likely reasons for the marked difference in their intratumoral spatial distribution. Together, these results strongly indicate that the pH-triggered disassembly of histidine-rich ELP_{BC}s leads to enhanced tumor penetration and a more uniform distribution throughout the tumor cross-section as compared to pH-insensitive ELP_{BC} micelles.

NIH-PA Author Manuscript

NIH-PA Author Manuscript

NIH-PA Author Manuscript

These results suggest that at early time points, as the nanoparticles first begin to accumulate in the tumor, the pH-insensitive particles encounter a barrier to diffusion and concentrate in the perivascular space while the pH-sensitive particles rapidly dissociate, increasing the diffusivity of the individual polymer chains and lessening their susceptibility to outward convection driven by elevated interstitial fluid pressure. Over time, the pH-insensitive micelles disassemble to some extent due to the dynamic nature of self-assembly and due to the decrease in the local concentration below the CMC, and this disassembly coupled with gradual diffusion allows these polymers to distribute better throughout the tumor volume, although focal sites of concentration remain. Meanwhile, the pH-sensitive polymer develops some concentrated regions over time, potentially because the rate of accumulation in the perivascular space in those regions exceeds their rate of transport into the tumor.

pH-sensitive liposomes were the first class of materials synthesized to approach the range of pH sensitivity required for intratumoral delivery of therapeutic or imaging cargo. While these carriers have achieved impressive specificity of release between pH 7.4 and 6.0[26] and have been successfully used to improve the intracellular delivery of a cytotoxic protein[27] and plasmid DNA,[28] pH-sensitive liposomes suffer from poor serum stability,[29] and incorporation of a stealth polymer at their exterior considerably reduced their pH sensitivity at the tumor extracellular pH.[29] Thirty years after the first pH-sensitive liposome was designed to release its contents in response to the low tumor extracellular pH,[26] no polymer nanoparticle has convincingly demonstrated this ability.

While a variety of pH-sensitive polymer systems have been developed to release drugs at low pH through mechanisms including acid-labile linkers,[2,30,31] low pH-induced interactions with the lipid membrane,[32-34] a solubility transition based on the polymer backbone itself[35] or hydrolytic cleavage of sidechains,[36,37] and others,[38,39] the vast majority of these systems are only responsive when the pH drops more than 2 pH units from ~7 to endosomal levels (≤5), and it remains a significant challenge to design polymers that can undergo a phase transition in the ≤ 1 pH unit difference that exists between normal tissues (7.2-7.4) and solid tumors (6.2-6.9). Furthermore, most of these polymers were not designed to form nanoparticles by self-assembly. Prior to this study, the only other self-assembling polymers that we know of that were designed to respond to tumor pH are a series of poly(L-histidine)/PEG block copolymers that were designed to form micelles that are destabilized at low pH.[40,41] Despite promising *in vivo* results including enhanced tumor growth delay for MCF-7 and drug-resistant MCF-7^{R} tumors,[42] these studies have not demonstrated a convincing alteration in the distribution of drug within the tumor, raising the possibility that these *in vivo* effects were due to an endosomal rather than an extracellular pH response. Second, the micelles in these studies existed as associated complexes that increased in size upon a decrease in pH,[43] raising uncertainty as to the nature of this material transition.

The His-containing ELP_{BC} $[VG_7A_8]$-80/$[VH_4]$-100 described here is a triple stimulus-responsive polymer that responds to temperature, pH and transition metal ions in a physiologically relevant range of temperature, pH and Zn^{2+} concentration. Self-assembly of unimers into micelles can be triggered by temperatures ranging from 32 to 40 °C, or by the addition of Zn^{2+} over an even wider range of temperature ranging from 5 to 50 °C. The addition of physiological levels of Zn^{2+} not only broadens the range of temperature over which self-assembly occurs, but also increases the stability of the micelle. pH provides an independent trigger to disassemble these micelles, as even a 1 pH unit drop from 7.4 to 6.4 results in the rapid disassembly of the micelles into unimers. The micelle disassembly at low pH observed *in vitro* translates to a visually arresting and statistically significant increase in the homogeneity of tumor distribution and the extent of tumor penetration. This improvement in the penetration of a nanoparticle through a solid tumor in a relatively short time (~4 h) may enable improved therapeutic efficacy by allowing covalently conjugated or

NIH-PA Author Manuscript

NIH-PA Author Manuscript

NIH-PA Author Manuscript

physically encapsulated drugs or imaging agents to reach and then treat or image interior tumor regions that are frequently inaccessible because of their higher interstitial pressure and lack of functional vasculature due to necrosis.[8] Efforts to develop this drug carrier into a therapeutic delivery system should begin with radiotherapeutics due to their simple conjugation and rapid action. Short half-life radionuclides or modifications to the system to facilitate cell entry of conjugated chemotherapeutics could convert the early improvement in tumor penetration into a significant enhancement of therapeutic efficacy. While the correlation between improved penetration and therapeutic efficacy will be drug- and delivery system-dependent, a recent paper suggests that addressing the critical issue of penetration[44] can indeed improve therapeutic efficacy,[45] and this new pH-sensitive system provides an excellent system to further test this hypothesis.

In conclusion, this paper presents the first demonstration of a pH-responsive genetically encoded polypeptide nanoparticle designed to dissociate in the mildly acidic conditions that prevail in the extracellular region of many solid tumors, and illustrates how pH-triggered disassembly of a polypeptide micelle within a tumor may provide a promising new avenue to improve the delivery of micellar –drug or imaging agent– cargo to solid tumors.

Supplementary Material

Refer to Web version on PubMed Central for supplementary material.

Acknowledgments

The authors acknowledge molecular biology assistance from John Andrew Pura and Andrew Sobel. This work was supported by NIH grant number R01EB007205 (A.C.), the Triangle MRSEC through NSF DMR, an NSF-sponsored IGERT fellowship to D.J.C. through grant number NSF-DGE-02-21632, and the Center for Interventional Oncology in the Intramural Research Program of the NIH.

References

(1). Matsumura Y, Maeda H. Cancer Res. 1986; 46:6387. [PubMed: 2946403]

(2). MacKay JA, Chen M, McDaniel JR, Liu W, Simnick AJ, Chilkoti A. Nat. Mat. 2009; 8:993.

(3). Greish K, Nagamitsu A, Fang J, Maeda H. Bioconj. Chem. 2005; 16:230.

(4). Greish K, Sawa T, Fang J, Akaike T, Maeda H. J. Control. Release. 2004; 97:219. [PubMed: 15196749]

(5). Matsumura Y. Jpn. J. Clin. Oncol. 2008; 38:793. [PubMed: 18988667]

(6). Nakanishi T, Fukushima S, Okamoto K, Suzuki M, Matsumura Y, Yokoyama M, Okano T, Sakurai Y, Kataoka K. J. Control. Release. 2001; 74:295. [PubMed: 11489509]

(7). Dreher MR, Liu W, Michelich CR, Dewhirst MW, Yuan F, Chilkoti A. J. Natl. Cancer Inst. 2006; 98:335. [PubMed: 16507830]

(8). Jain RK. Adv. Drug Deliv. Rev. 2001; 46:149. [PubMed: 11259838]

(9). Cardone RA, Casavola V, Reshkin S. J. Nat. Rev. Cancer. 2005; 5:786.

(10). Urry DW. J. Phys. Chem. B. 1997; 101:11007.

(11). Dreher MR, Simnick AJ, Fischer K, Smith RJ, Patel A, Schmidt M, Chilkoti A. J. Am. Chem. Soc. 2008; 130:687. [PubMed: 18085778]

(12). Pattanaik A, Gowda DC, Urry DW. Biochem. Biophys. Res. Commun. 1991; 178:539. [PubMed: 1859415]

(13). Lim DW, Nettles DL, Setton LA, Chilkoti A. Biomacromolecules. 2007; 8:1463. [PubMed: 17411091]

(14). MacKay JA, Callahan DJ, FitzGerald KN, Chilkoti A. Biomacromolecules. 2010; 11:2873.

(15). Meyer DE, Chilkoti A. Biomacromolecules. 2004; 5:846. [PubMed: 15132671]

(16). Meyer DE, Chilkoti A. Biomacromolecules. 2002; 3:357. [PubMed: 11888323]

NIH-PA Author Manuscript

NIH-PA Author Manuscript

NIH-PA Author Manuscript

(17). Luscombe NM, Austin SE, Berman HM, Thornton JM. Genome Biol. 2000; 1:1. [PubMed: 11178226]

(18). Klemba M, Regan L. Biochemistry. 1995; 34:10094. [PubMed: 7632681]

(19). Hofmeister F. Arch. Exp. Path. Pharm. 1888; 24:247.

(20). Meyer DE, Chilkoti A. Biomacromolecules. 2004; 5:846. [PubMed: 15132671]

(21). Trumbo P, Yates AA, Schlicker S, Poos M. J. Am. Diet. Assoc. 2001; 101:294. [PubMed: 11269606]

(22). Kasperek K, Feinendegen LE, Lombeck I, Bremer H. J. Eur. J. Pediatr. 1977; 126:199.

(23). Antonietti M, Heinz S, Schmidt M, Rosenauer C. Macromolecules. 1994; 27:3276.

(24). Kuin A, Smets L, Volk T, Paans A, Adams G, Atema A, Jahde E, Maas A, Rajewsky MF, Visser G, Wood P. Cancer Res. 1994; 54:3785. [PubMed: 8033098]

(25). Dreher MR, Simnick AJ, Fischer K, Smith RJ, Patel A, Schmidt M, Chilkoti A. J Am Chem Soc. 2008; 130:687. [PubMed: 18085778]

(26). Yatvin MB, Kreutz W, Horwitz BA, Shinitzky M. Science. 1980; 210:1253. [PubMed: 7434025]

(27). Connor J, Huang L. Cancer Res. 1986; 46:3431. [PubMed: 2871923]

(28). Wang C-Y, Huang L. Biochemistry. 1989; 28:9508. [PubMed: 2558722]

(29). Liu D, Huang L. Biochim. Biophys. Acta. 1990; 348

(30). Bae Y, Fukushima S, Harada A, Kataoka K. Angew. Chem. Int. Ed. 2003; 42:4640.

(31). Bae Y, Jang WD, Nishiyama N, Fukushima S, Kataoka K. Mol. Biosyst. 2005; 1:242. [PubMed: 16880988]

(32). Li W, Nicol F, Szoka FC Jr. Adv. Drug Del. Rev. 2004; 56:967.

(33). Murthy N, Robichaud JR, Tirrell DA, Stayton PS, Hoffman AS. J. Control. Release. 1999; 61:137. [PubMed: 10469910]

(34). Reshetnyak YK, Andreev OA, Lehnert U, Engelman DM. Proc. Natl. Acad. Sci. U.S.A. 2006; 103:6460. [PubMed: 16608910]

(35). Potineni A, Lynn DM, Langer R, Amiji MM. J. Control. Release. 2003; 86:223. [PubMed: 12526819]

(36). Soga O, van Nostrum CF, Fens M, Rijcken CJF, Schiffelers RM, Storm G, Hennink WE. J. Control. Release. 2005; 103:341. [PubMed: 15763618]

(37). van Nostrum, CF.; Neradovic, D.; Soga, O.; Hennink, WE. Polymeric Micelles with Transient Stability: A Novel Delivery Concept. In: Svenson, S., editor. Polymeric Drug Delivery I. American Chemical Society; Washington, D.C.: p. 40

(38). Rijcken CJF, Soga O, Hennink WE, van Nostrum CF. J. Control. Release. 2007; 120:131. [PubMed: 17582642]

(39). Asokan A, Cho MJ. J. Pharm. Sci. 2002; 91:903. [PubMed: 11948528]

(40). Lee ES, Shin HJ, Na K, Bae YH. J. Control. Release. 2003; 90:363. [PubMed: 12880703]

(41). Lee ES, Na K, Bae YH. J. Control. Release. 2003; 91:103. [PubMed: 12932642]

(42). Lee ES, Na K, Bae YH. J. Control. Release. 2005; 103:405. [PubMed: 15763623]

(43). Yin H, Lee ES, Kim D, Lee KH, Oh KT, Bae YH. J. Control. Release. 2008; 126:130. [PubMed: 18187224]

(44). Minchinton AI, Tannock IF. Nat. Rev. Cancer. 2006; 6:583. [PubMed: 16862189]

(45). Jang B-S, Lee S-M, Kim HS, Shin IS, Razjouyan F, Wang S, Yao Z, Pastan I, Dreher MR, Paik CH. Nucl. Med. Biol. 2012 in press.

NIH-PA Author Manuscript

NIH-PA Author Manuscript

NIH-PA Author Manuscript

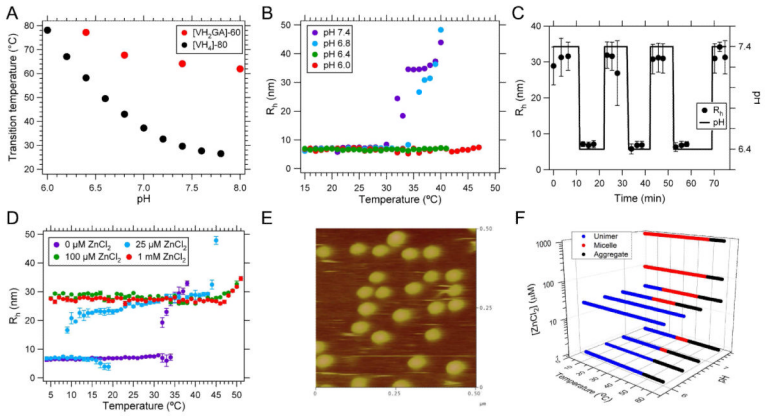

Figure 1.

Material properties of histidine-rich ELPs and ELP_{BC}s. (A) The T_t of histidine-containing single block ELPs over a range of pH measured by temperature-programmed turbidimetry. (B) R_h of ELP_{BC} $[VG_7A_8]$-80/$[VH_4]$-100 as a function of temperature at various pHs. (C) R_h of ELP_{BC} $[VG_7A_8]$-80/$[VH_4]$-100 as a function of isothermal (37 °C) pH cycling between 7.4 and 6.4. (D) R_h for the same ELP_{BC} as in (B) and (C) as a function of temperature at pH 7.4 with different concentrations of $ZnCl_2$ added in the range of 0-1 mM. (E) Tapping mode AFM image in buffer of zinc stabilized micelles of $[VG_7A_8]$-80/$[VH_4]$-100 at 25 °C and pH 7.4. (F) Phase diagram of the ELP_{BC} $[VG_7A_8]$-80/$[VH_4]$-100. Note: data in the absence of $ZnCl_2$ are plotted at 1 μM $ZnCl_2$ to enable presentation on a log scale. The different colored regions of the 3-D plot represents the ranges of stimulus combinations (temperature, pH and Zn^{2+} concentration) at which the Histidine-rich ELP_{BC} exists as a unimer (blue), micelle (red), or aggregate (black).

NIH-PA Author Manuscript

NIH-PA Author Manuscript

NIH-PA Author Manuscript

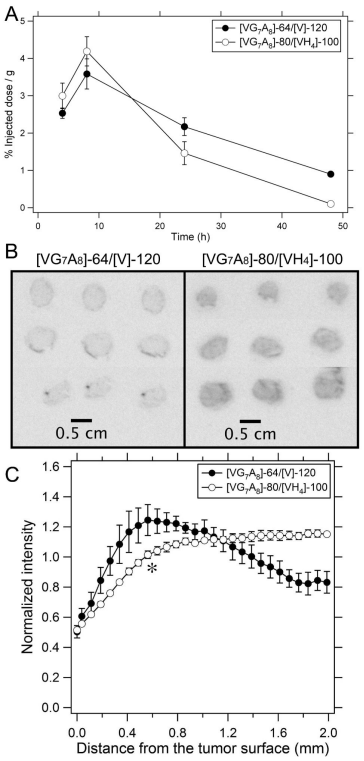

Figure 2.

In vivo behavior of His-free and His-rich ELP_{BC}s. (A) The tumor accumulation of His-free and His-rich ELP_{BC}s were measured 4, 8, 24, and 48 h after *i.v.* administration of ^{125}I-labeled polymers into nude mice bearing HCT-15 human colon adenocarcinomas. (B) Autoradiographic imaging of tumor sections from mice collected 4 h after injection with the two polymers. Note that raw intensities should not be compared due to a difference in the degree of labeling between the two polymers. (C) Mean normalized intensity 4 h after injection across the tumor cross-section.

NIH-PA Author Manuscript

NIH-PA Author Manuscript

NIH-PA Author Manuscript

Table 1

Critical micelle concentration of ELP [VG_7A_8]-80/[VH_4]-100 measured by pyrene fluorescence.*

	0 μM $ZnCl_2$	**100 μM $ZnCl_2$**	**1 mM $ZnCl_2$**
pH 8.0	23.7 ± 4.2 μM	6.4 ± 1.8 μM	**
pH 7.4	32.6 ± 3.8 μM	8.9 ± 3.0 μM	4.5 ± 0.3 μm

* Values represent mean ± SE.

** 1 mM $ZnCl_2$ precipitated in pH 8.0 HEPES, so CMC could not be measured under these conditions.

NIH-PA Author Manuscript NIH-PA Author Manuscript NIH-PA Author Manuscript

Table 2

Static light scattering of 50 μM ELP [VG_7A_8]-80/[VH_4]-100 in 10 mM HEPES and 140 mM NaCl and different concentrations of $ZnCl_2$. R_h is the hydrodynamic radius, R_g is the radius of gyration, ρ is R_g/R_h, the MW is that of the self-assembled micelles, and Z is the coordination number (average number of polymer chains per micelle).

Temperature (°C)	[$ZnCl_2$] (μM)	R_h (nm)	R_g (nm)	ρ	MW (kDa)	Z*
37	0	31.9	19.9	0.623	3269	44
37	25	29.6	14.7	0.495	5366	73
25	25	31.1	16.1	0.517	5271	70

*Apparent coordination numbers (without CMC correction).